Theoretical study of the elution profile of a high-concentration sample anion in non-suppressed ion chromatography

Kyoko Ando[a,*], Atsushi Yamamoto[b], Masayuki Nishimura[c], Kazuichi Hayakawa[a]

[a]*Faculty of Pharmaceutical Sciences, Kanazawa University, 13-1, Takara-machi, Kanazawa 920, Japan*
[b]*Toyama Institute of Health, 17-1, Nakataikoyama, Kosugi-machi, Toyama 939-03, Japan*
[c]*Shimadzu Scientific Instruments, Inc., 7102 Riverwood Drive, Columbia, MD 21046, USA*

Abstract

In non-suppressed ion chromatography, an injection of a high concentration analyte on an anion-exchange column results in the leading and broadening of the peaks. The mechanism was elucidated by analyses of the behavior of various components on the elution model. When the analyte concentration was high, a large amount of eluent was expelled from the stationary phase. Subsequently the eluent concentration in the analyte band decreased. This resulted in a distortion of the analyte peak shape. The use of a large buffer capacity of the mobile phase to avoid the distortion is discussed. The distortion practically disappeared when a mobile phase was buffered with a high concentration glycine.   © 1997 Elsevier Science B.V.

Keywords: Mobile phase composition; Peak shape; Chloride; Inorganic anions

1. Introduction

Ion chromatography (IC) has become an accurate and sensitive method for the separation and determination of ionic compounds. Although IC is generally used for the analysis of anions in various environmental samples (e.g., river water, rain water), it is difficult to determine low and high concentration anions simultaneously in high salinity samples (e.g., sea water, oilfield water) [1–3]. One reason for this is that an undiluted or slightly diluted sample containing high concentration analytes causes the leading and/or broadening of the peaks. This distortion results in the loss of the ability to quantitate and results in errors of identification. Another reason is that the lower concentration anion peaks are frequently masked by the higher concentration peaks.

The distortion and masking can be avoided by using a more highly diluted sample, but this makes the determination of the lower concentration anions impracticable. These problems are more frequently observed in non-suppressed IC (NS-IC) than in suppressed IC.

Guiochon et al. [4] showed that the distortion arises from the nonlinearity of the equilibrium isotherm of the solute between the mobile and the stationary phases in liquid chromatography (LC) including the reversed-phase mode. But this theory is not always applicable to IC in the ion-exchange mode because of the difference in the retention mechanism. The aim of this work is to clarify the mechanism of distortion of a high concentration analyte peak in NS-IC by comparing experimental and simulated results using our elution model based on plate theory [5–7]. An effective method for avoiding the distortion is also proposed.
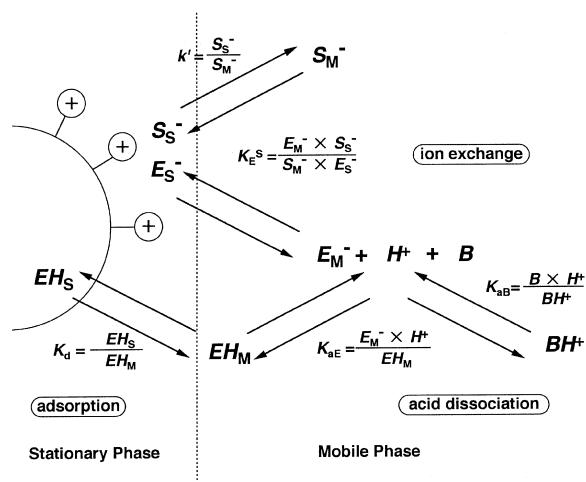

Fig. 1. Equilibrium reactions introduced to the elution model.

2. Theory

All equilibrium reactions in our elution model are shown in Fig. 1. We dealt with the several reactions (ion-exchange, acid dissociation, and adsorption) of the eluent (E_M^-, EH_M, E_S^-, EH_S), the analyte (S_M^-, S_S^-), and the buffer (B, BH^+) in the elution model. Explanations of the variables appear in Fig. 1 and the following calculations are listed in Appendix A. For this model, we made several assumptions. (1) The model is based on plate theory, and all equilibrium reactions are completed in each theoretical plate. (2) The phase ratio of the column is unity. (3) The buffer in the mobile phase does not interact (either through ion-exchange or adsorption) with the stationary phase. (4) The analyte and the dissociated eluent are monovalent.

Using the above assumptions, the following equations were formed.

The total amount of the eluent (TE), the buffer (TB) and the analyte (TS) on a plate are defined as

$$TE = E_M^- + EH_M + E_S^- + EH_S$$
$$= E_M^- + (1 + K_d)EH_M + E_S^- \tag{1}$$

$$TB = B + BH^+ \tag{2}$$

$$TS = S_M^- + S_S^- \tag{3}$$

where K_d is the distribution coefficient of the undissociated form of the eluent.

The dissociation constants of the eluent (K_{aE}) and the buffer (K_{aB}) are

$$K_{aE} = H^+ \cdot E_M^- / EH_M \tag{4}$$

$$K_{aB} = H^+ \cdot B / BH^+ \tag{5}$$

Eqs. (1) and (4) give

$$E_M^- = (TE - E_S^-)K_{aE} / [H^+(1 + K_d) + K_{aE}] \tag{6}$$

Eqs. (2) and (5) give

$$BH^+ = TB \cdot H^+ / (K_{aB} + H^+) \tag{7}$$

The charge balance of the mobile phase is described as

$$E_M^- + S_M^- = BH^+ + H^+ + Na^+ \tag{8}$$

where Na^+ represents the amount of the counter cation of the analyte (sodium ion) on a plate.

The charge balance of the stationary phase is described as

$$IECap = E_S^- + S_S^- \tag{9}$$

where $IECap$ represents the ion-exchange capacity per theoretical plate.

The affinity of the analyte for ion-exchange sites of the column (K_E^S) is expressed by the following formula:

$$K_E^S = E_M^- \cdot S_S^- / (E_S^- \cdot S_M^-) \tag{10}$$

The amount of the dissociated eluent in the stationary phase on a plate (E_S^-) is calculated from Eqs. (2), (3), (8)–(10) by using a given H^+.

$$E_S^- 1/2\{B \pm \sqrt{[B^2 - 4(K_E^S - 1)IECap \cdot A]}\}/(K_E^S - 1) \tag{11}$$

where $A = TS - Na^+ - TB \cdot H^+ / (K_{aB} + H^+) - H^+ - IECap$ and $B = A - IECap - K_E^S(TS - IECap)$.

The amount of the analyte in the mobile phase, S_M^-, is calculated from Eqs. (4) and (6) and E_S^-.

Eqs. (6)–(8) give

$$(1 + K_d)(H^+)^3 + [(1 + K_d)C + K_{aE}](H^+)^2 + [(1 +$$

$$K_d)K_{aB}(Na^+ - S_M^-) + (C - TE + E_S^-)K_{aE}]H^+ +$$

$$K_{aB}K_{aE}(Na^+ - TE + E_S^- - S_M^-) = 0 \qquad (12)$$

where $C = Na^+ + TB + K_{aB} - S_M^-$.

A more accurate value for H^+ can be calculated from Eq. (12). To obtain the final E_S^- and H^+ on a plate, the calculation of Eqs. (11) and (12) were repeated until these values converged. The final H^+ on the ith plate was taken as the initial H^+ on the $(i+1)$th plate in this calculation.

In this model, plotting the difference between the conductivity due to E_M^- and that due to S_M^- on the last theoretical plate versus capacity factor was used to simulate a chromatogram.

3. Experimental

3.1. Instrumentation and reagents

The ion chromatograph consisted of an LC-10AD pump, a CTO-6AS column oven, a CDD-6A electrical conductivity detector (Shimadzu, Kyoto, Japan), a Model 7125 manual injector (Rheodyne, Cotati, CA, USA) and an U-228 recorder (Nippon Denshi Kagaku, Tokyo, Japan). The analytical column was a Shim-pack IC-A3 ($d_p = 5$ μm, 150 mm×4.6 mm I.D.) anion-exchange column (Shimadzu, Kyoto, Japan). Pure water was prepared with a Milli-QII system (Millipore, Bedford, MA, USA). All chemicals used were analytical-reagent grade.

3.2. Preparation of mobile phase and analytical conditions

An 8 mM aqueous solution of p-hydroxybenzoic acid (p-PBA) was prepared by dissolving a weighed amount of the substance in pure water. Two aliquots were taken; one was adjusted to pH 4.4 with sodium hydroxide (MP 1) and the other was adjusted to the same pH value with 300 mM glycine (MP 2). The column was maintained at 40°C, and the conductivity detector cell at 43°C. For all runs, the mobile phase was delivered at 1.2 ml/min. Analytes were chloride ion solutions at various concentrations. Injection volume was 5 μl.

4. Results and discussions

4.1. Characteristics of the distortion

An experimental chromatogram of 1 mM sodium chloride is shown in Fig. 2a. The retention time, the peak width and the leading factor (defined as the ratio of the width of the leading edge of the peak to the width of the tailing edge) of the chloride ion peak were 4.7 min, 0.6 min and 0.7, respectively. When a 100 mM sodium chloride solution was injected, the peak shape was leaded and broadened (Fig. 2b). The retention time, the peak width and the leading factor of the peak increased to 5.5 min, 1.5 min and 4.2, respectively.

The peak heights of various concentrations of chloride ion relative to the peak height of 1 mM chloride ion are shown in Fig. 3 (top). The relative peak height did not increase linearly and was only 35 for 100 mM chloride ion. Thus, the lack of linearity made it difficult to quantitate chloride ion at higher concentration by the peak height technique. The peak shape was also distorted by higher chloride ion concentrations (Fig. 3, bottom). Though the effective ion-exchange capacity of the Shim-pack IC-A3 column was about 30 μequivalents, the injection of only 30 mM sodium chloride (150 nequivalents chloride ion) resulted in a leading factor of 1.7. Evidently, the distortion occurred, when a small part
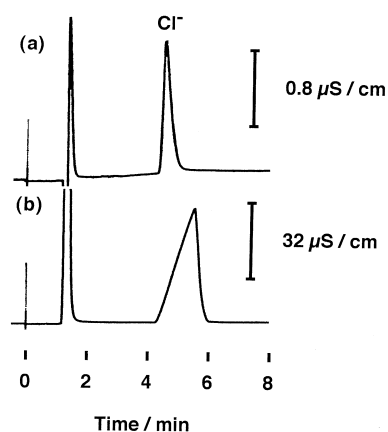

Fig. 2. Experimental chromatograms of 1 mM (a) and 100 mM (b) chloride ion. The mobile phase is MP 1 and other conditions are described in Section 3.
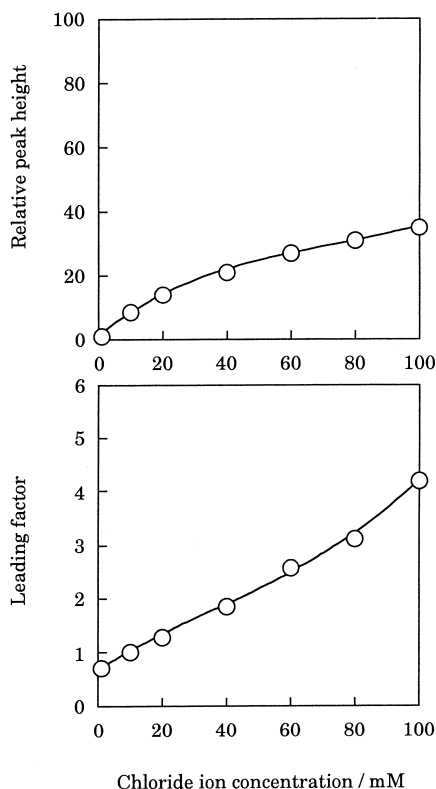
Fig. 3. Experimentally observed relative peak height and leading factor versus chloride ion concentration in chromatograms. The mobile phase is MP 1 and other conditions are described in Section 3.

of ion-exchange sites of the column was occupied with chloride ions.

4.2. The mechanism of distortion

The influences of several parameters on the elution profile in our model were studied to clarify the mechanism of distortion. The injection volume and pH value of the mobile phase used in the model were the same as those in the experiment. The capacity factor of the analyte, K_{aB}, the theoretical plate number and the ion-exchange capacity of the column were set at 3.0, $1.0 \cdot 10^{-14}$, 100 and 32.5 μequivalents, respectively.

First, the simple elution model was used: the ion-exchange reaction occurred according to the capacity factor of the analyte ($k' = S_S^- / S_M^-$) instead of Eq. (10), all eluent species were dissociated ($K_{aE} =$
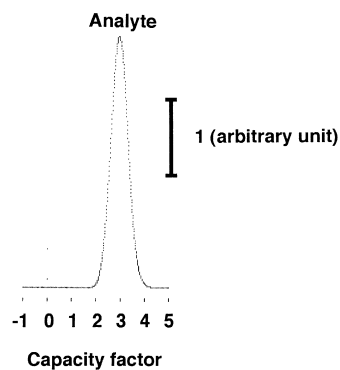

Fig. 4. Simulated chromatogram of 100 mM analyte obtained by the first model.

1), and the buffer capacity of the mobile phase was very low. The simulated chromatogram of a 100 mM analyte solution is shown in Fig. 4. Based on this model, no distortion was observed even if the analyte concentration was over 500 mM. Moreover, the retention time decreased with an increase in the analyte concentration.

Second, the ion-exchange reaction according to Eq. (10) was incorporated in the model in which the other parameters were the same as in the first model. The simulated chromatograms of 1 mM and 100 mM analyte solutions are shown in Fig. 5a and 5b, respectively. The leading and broadening analyte peak was observed in the simulated chromatogram of 100 mM analyte. The leading factor and the relative peak height versus analyte concentration are shown
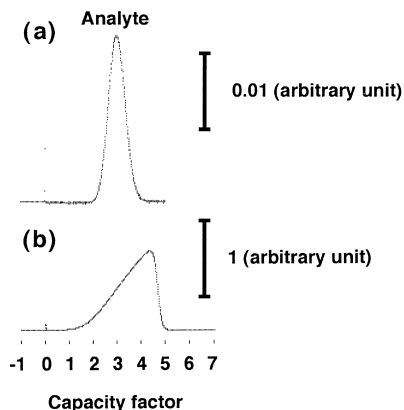

Fig. 5. Simulated chromatograms of 1 mM (a) and 100 mM (b) analyte obtained by the second model.

in Fig. 6 (open circles). The leading factors increased with increasing analyte concentration. The relative peak height curve in Fig. 6 (top) was almost the same as that shown in Fig. 3.

We analyzed the behavior of each component in the column based on the second model and propose the following mechanism for the distortion. After the injection of the high concentration analyte, the eluent is expelled from the stationary phase. At the same time, the expelled eluent forms the solvent front, and the eluent concentration in the analyte band decreases considerably (Fig. 7). The elution power of the mobile phase, i.e., the migration rate of the analyte decreases at the trough of E_M^-. A symmetric distribution of S_M^- is distorted by the difference in

Fig. 7. A speculated distortion mechanism of the analyte profile. The lengths of the dashed arrows and the solid arrows indicate the elution power of the mobile phase and the migration rate of the analyte in the column.

the migration rate of the analyte, which is expressed by the lengths of the solid arrows in Fig. 7, and the leading peak is formed.

Third, we set K_{aE} at $2.6 \cdot 10^{-5}$ to result in the presence of both dissociated and undissociated eluent species in the model using a weak acid eluent, which is generally used in NS-IC. Fig. 5 also shows the leading factor and the relative peak height versus analyte concentration from the third model (closed circles). The curves were almost the same as those in Fig. 3, and the distortion obtained from the third model was greater than that of the second model (open circles).

Using the weak acid eluent (the third model), the pH value of the analyte band is decreased by the injection of the high concentration analyte. The undissociated eluent is adsorbed on the stationary phase and the eluent concentration in the mobile phase of the analyte band decreases more than it does in the second model. The greater distortion results from the greater decrease in the eluent concentration.

4.3. A method for avoiding the distortion

If the pH is kept constant in spite of the decrease in the eluent concentration in the analyte band, the undissociated species, which are released into the mobile phase, become dissociated. Then the eluent
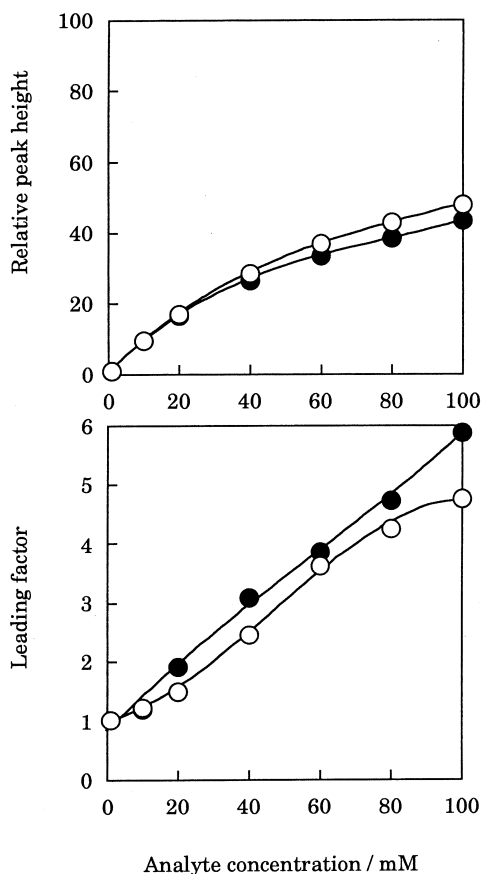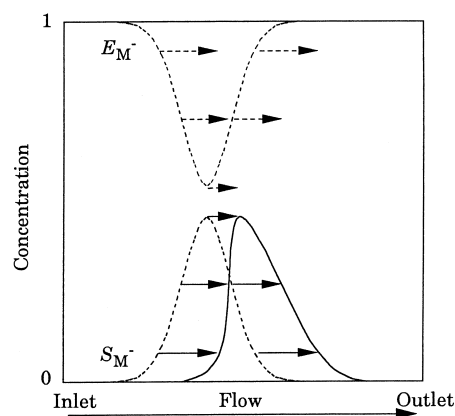

Fig. 6. Simulated relative peak height and leading factor versus analyte concentration in chromatograms. Open and closed circles represent the values obtained from the second and third models, respectively.

concentration can recover. A large buffer capacity of the mobile phase might be effective in preventing the distortion.

So, we set K_{aB} of the buffer in the mobile phase at $3.8 \cdot 10^{-3}$ to give a large buffer capacity in the final model. The simulated chromatogram of 100 mM analyte is shown in Fig. 8. The leading factor and the relative peak height versus analyte concentration are shown in Fig. 9 (open circles). The leading factor of 100 mM analyte was 1.8, and the linearity between the peak height and the analyte concentration was slightly improved.

We previously studied glycine as a modifier for controlling the retention time of the system peak when phthalic acid eluent was used [8]. Glycine was also chosen in this study as the buffer because of its suitable pK_{a1} and high solubility. The mobile phase containing 300 mM glycine (MP 2) has about three times the buffer capacity of the mobile phase adjusted to pH 4.4 with sodium hydroxide (MP 1). An experimental chromatogram of 100 mM sodium chloride utilizing MP 2 is shown in Fig. 10. The leading factor and the relative peak height versus chloride ion concentration are also shown in Fig. 9 (closed circles). The relative peak height was almost proportional to the chloride ion concentration, and the leading factor was nearly 1. The distortion practically disappeared. Under these conditions the peak area of the analyte was always larger than that obtained using the mobile phase with a smaller buffer capacity (MP 1), since the eluent concentration was not changed by the injection of high concentration sodium chloride. The most important result is that the large buffer capacity of the mobile
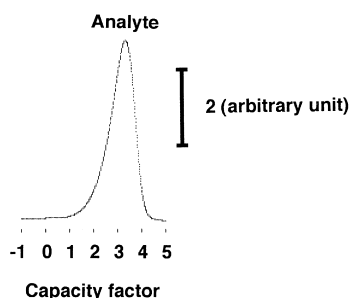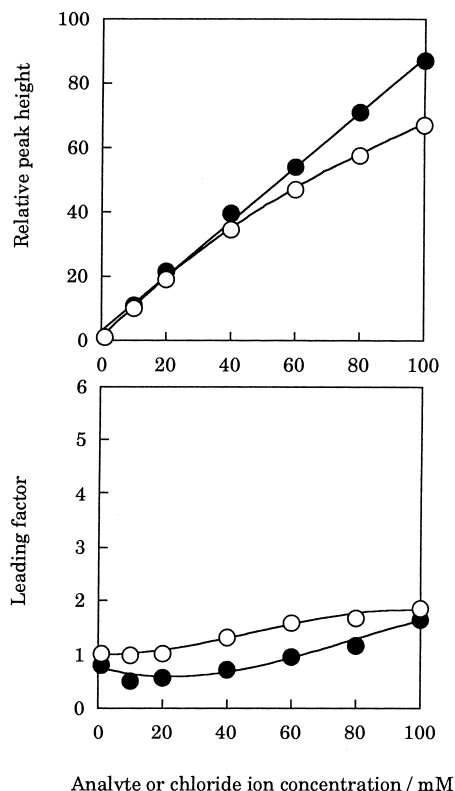

Fig. 9. Relative peak height and leading factor versus analyte concentration in simulated chromatograms (open circles) and in experimentally observed chromatograms (closed circles) using a mobile phase with a large buffer capacity. The mobile phase is MP 2 and other conditions are described in Section 3.

phase avoids the distortion that occurs in NS-IC by the injection of high concentration analyte.

It is known that the peak height of sulfate is decreased by the injection of high concentration chloride ion not only in suppressed IC [9] but also in NS-IC [10]. We have started a theoretical investigation on this phenomenon utilizing the proposed model.

Appendix A

Symbols

B amount of dissociated buffer in mobile phase on a plate of column

Fig. 8. Simulated chromatogram of 100 mM anayte obtained by the final model.
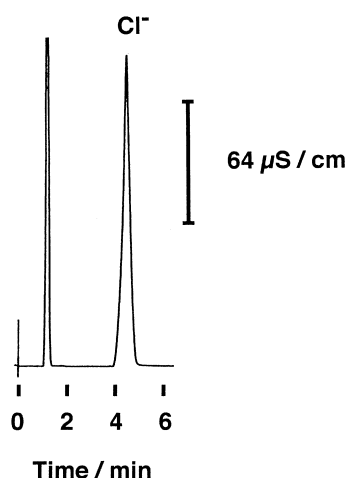
Fig. 10. Experimental chromatograms of 100 mM chloride ion using a mobile phase with large buffer capacity. The mobile phase is MP 2 and other conditions are described in Section 3.

BH^+ amount of undissociated buffer in mobile phase on a plate of column

E_M^- amount of dissociated eluent in mobile phase on a plate of column

EH_M amount of undissociated eluent in mobile phase on a plate of column

E_S^- amount of dissociated eluent in stationary phase on a plate of column

EH_S amount of undissociated eluent in stationary phase on a plate of column

$IECap$ ion-exchange capacity per theoretical plate

k' capacity factor of analyte

K_{aB} dissociation constant of buffer in the mobile phase

K_{aE} dissociation constant of eluent

K_d distribution coefficient of undissociated eluent

K_E^S affinity of analyte for ion-exchange sites of column

Na^+ amount of counter cation of analyte (sodium ion) on a plate of column

S_M^- amount of analyte in mobile phase on a plate of column

S_S^- amount of analyte in stationary phase on a plate of column

TB total amount of buffer on a plate of column

TE total amount of eluent on a plate of column

TS total amount of analyte on a plate of column

References

[1] R.P. Sigh, N.M. Abbas, S.A. Smesko, J. Chromatogr. A 733 (1996) 73.

[2] R. Salasauvert, J. Colmenarez, H. Deledo, M. Colina, E. Gutierrez, A. Bravo, L. Soto, S. Azuero, J. Chromatogr. A 706 (1995) 183.

[3] R. Kadnar, J. Rieder, J. Chromatogr. A 706 (1995) 301.

[4] J. Guiochon, S. Golshan-Shirazi, A. Jaulmes, Anal. Chem. 60 (1988) 1856.

[5] A. Yamamoto, A. Matsunaga, M. Ohto, E. Mizukami, K. Hayakawa, M. Miyazaki, J. Chromatogr. 482 (1989) 145.

[6] A. Yamamoto, K. Hayakawa, A. Matsunaga, M. Ohto, E. Mizukami, M. Miyazaki, J. Chromatogr. 627 (1992) 17.

[7] M. Nishimura, M. Hayashi, A. Yamamoto, K. Hayakawa, M. Miyazaki, Anal. Sci. 11 (1995) 755.

[8] M. Nishimura, M. Hayashi, A. Yamamoto, T. Horikawa, K. Hayakawa, M. Miyazaki, J. Chromatogr. A 708 (1995) 195.

[9] R.P. Singh, E.R. Pambid, N.M. Abbas, Anal. Chem. 63 (1991) 1987.

[10] M. Tsuji, M. Hayashi, M. Matsuoka, T. Takamitsu, Eisei Kagaku 42 (1996) 96.